Carbohydrate Polymers 245 (2020) 116547

Contents lists available at ScienceDirect

Carbohydrate Polymers

journal homepage: www.elsevier.com/locate/carbpol

Synthesis of bioactive silver nanoparticles using alginate, fucoidan and laminaran from brown algae as a reducing and stabilizing agent

Y.A. Yugay[a], R.V. Usoltseva[b], V.E. Silant'ev[c], A.E. Egorova[a,d], A.A. Karabtsov[e], V.V. Kumeiko[d,f], S.P. Ermakova[b], V.P. Bulgakov[a], Y.N. Shkryl[a,*]

[a] Federal Scientific Center of the East Asia Terrestrial Biodiversity, Far Eastern Branch of the Russian Academy of Sciences, Vladivostok, 690022, Russia
[b] G.B. Elyakov Pacific Institute of Bioorganic Chemistry, Far Eastern Branch of the Russian Academy of Sciences, Vladivostok, 690022, Russia
[c] Institute of Chemistry, Far Eastern Branch of the Russian Academy of Sciences, Vladivostok, 690022, Russia
[d] Far Eastern Federal University, Vladivostok, 690950, Russia
[e] Far Eastern Geological Institute, Far Eastern Branch of the Russian Academy of Sciences, Vladivostok, 690022, Russia
[f] A.V. Zhirmunsky National Scientific Center of Marine Biology, Far Eastern Branch of the Russian Academy of Sciences, Vladivostok, Russia

ARTICLE INFO

Keywords:
Green synthesis
Nanosilver
Cytotoxicity
Antibacterial activity
Saccharina cichorioides
Fucus evanescens

ABSTRACT

In this report, polysaccharides – alginate, fucoidan, laminaran – were isolated from marine algae *Saccharina cichorioides* and *Fucus evanescens* and their activity as a reducing and stabilizing agents in the biogenic synthesis of silver nanoparticles was evaluated. The cytotoxic and antibacterial properties of obtained nanoparticles were also assessed. It was found that all tested polysaccharides could be used as a reducing agent; however, their catalytic activities varied significantly in the following range alginate < fucoidan < laminaran. Nanoparticles demonstrated cytotoxicity against rat C6 glioma cells. It was considerably higher for alginate- and laminaran-obtained nanosilver samples compared to fucoidan. Additionally, silver nanoparticles possessed considerable antibacterial properties more pronounced in fucoidan-obtained samples. Our data demonstrate that different algal polysaccharides can be used for the synthesis of silver nanoparticles with varying bioactivities.

1. Introduction

Synthesis of metal nanoparticles is an important research area in nanotechnology because of their unusual size- and shape-dependent properties and attractive applications in medicine, catalysis, optoelectronics and biotechnology (Huang & Yang, 2004; Maneerung, Tokura, & Rujiravanit, 2008). Formation of metal nanoparticles can be achieved using top-down (i.e. from bulk materials) and bottom-up (i.e. from precursors) approaches by a variety of physical and chemical means (Gao & Cranston, 2008; Rodriguez-Sanchez, Blanco, & Lopez-Quinetela, 2000; Sailaja, Amareshwar, & Chakravarty, 2011). However, many of these methods use toxic reductants, extreme physical conditions, and are costly, non-eco-friendly and have low production yields (Gilaki, 2010). Therefore in recent years, the bioreduction of metal ions from their water-soluble precursors promoted by the extracts, by-products and individual compounds from different organisms is extensively studied as an alternative bottom-up method for synthesis of metal nanoparticles (Singh et al., 2018). This technology is also known as “green synt hesis”; it is easier to perform and cheaper than traditional approaches, doesn’t bear environmental risk while synthesized biogenic nanoparicles possess a broad spectrum of activities and can be employed in biological applications (Morones, Elechiguerra, Camacho, & Ramirez, 2005).

The most common way of green nanoparticle synthesis involves the use of water extracts from different organisms, including fungi (Balaji, Basavaraja, Bedre, Prabhakar, & Venkataraman, 2011), algae (Sahayaa, Rajesh, & Rahi, 2012) and plants (Amkamwar, Damle, Ahmad, & Sastry, 2005; Chandran, Chaudhary, Pasricha, Ahmad, & Sastry, 2006; Li et al., 2007; Shankar, Ahmad, & Sastry., 2003). The reduction of metal ions to the nanoparticles can occur extracellularly using bacteria, yeast and fungi cultures (Kowshik et al., 2002; Bhainsa & D’Souza, 2006; Saifuddin, Wong, & Nur Yasumira, 2009). Silver (Ag) and gold (Au), as well as their bimetallic particles, were the first to be produced by green synthesis. Still, later this technology extended to a spectrum of metals including copper (Cu) and copper oxide (CuO), zinc oxide (ZnO), cerium oxide (CeO_2), titanium dioxide (TiO_2), sulphide (CdS), iron oxide (Fe_2O_3), palladium (Pd) (Gour & Jain, 2019), and metalloids such as tellurium (Medina et al., 2019), selenium (Gunti, Dass, & Kalagatur,

* Corresponding author at: Federal Scientific Center of the East Asia Terrestrial Biodiversity of the Far East Branch of Russian Academy of Sciences, 159 Stoletija Str., Vladivostok, 690022, Russia.
E-mail address: yn80@mail.ru (Y.N. Shkryl).

https://doi.org/10.1016/j.carbpol.2020.116547
Received 25 March 2020; Received in revised form 9 May 2020; Accepted 31 May 2020
Available online 06 June 2020

2019), silicon (Tiwari et al., 2019), and even for the reduction of graphene oxide (Lee & Kim, 2014).

Using individual biomolecules as reductants and capping agents is another attractive approach in green synthesis of nanoparticles. These methods can potentially demonstrate more sustainable results in terms of particle size and shape distribution as soon as they lack the complexity of crude extracts or media composition, which are challenging to maintain precisely. For instance, silver nanoparticles were synthesized with total bacterial DNA (Chumpol & Siri, 2018), horseradish peroxidase (Schneidewind et al., 2012), nitrate reductase (Kumar et al., 2007), and sericin (Aramwit, Bang, Ratanavaraporn, & Ekgasit, 2014). Polysaccharides represent the major class of biological polymers in living organisms and have an outstanding reduction potential. In particular, chitosan, heparin, cellulose, and pectin facilitate biosynthesis of uniform silver and gold nanoparticles (Garza-Navarro et al., 2013; Huang & Yang, 2004; Tummalapalli, Deopura, Alam, & Gupta, 2015).

Brown algae are an abundant and easily renewable source of polysaccharides of interesting structure and physiological activity. Along with the well-known alginic acid, brown algae contain unique water-soluble polysaccharides – laminarans and fucoidans. The increased interest in these compounds is explained by the presence of a wide range of pharmacological properties, low toxicity and the possibility of using them for new-generation drugs (Li et al., 2019).

The ability to catalyze the formation of silver nanoparticles with antibacterial activity has been shown already for some polysaccharides from red, brown, and green algae (El-Rafie, El-Rafie, & Zahran, 2013; Venkatpurwar & Pokharkar, 2011). Seaweed polysaccharides have different properties and structure, so their reducing potential for the formation of metal nanoparticles could be significantly different also.

In this work, we present a simple and eco-friendly method for the preparation of silver nanoparticles using naturally-occurring polysaccharides from *F. evanescens* and *S. cichorioides*. They act as biocatalysts for the wet chemical reduction of silver ions and as the stabilizing agents for the produced biologically active Ag nanoparticles.

2. Experimental

2.1. Production and characterization of polysaccharides from brown algae

Laminaran (ScL) and fucoidan (ScF) from *S. cichorioides* and fucoidan (FeF) and alginate (FeA) from *F. evanescens* were obtained by the elaborate scheme described earlier (Sokolova, Ermakova, Awada, Zvyagintseva, & Kanaan, 2011). Total carbohydrates were quantified using the phenol-sulfuric acid method (Dubois, Gilles, Hamilton, Rebers, & Smith, 1956). The monosaccharide composition was determined by gas-liquid chromatography (GLC) after polysaccharide hydrolysis in 2 M trifluoroacetic acid (6 h, 100 °C) and production of alditol acetate derivatives. The number of sulfate groups was determined using the $BaCl_2$ gelatin method (Dodgson, 1961). NMR spectra were obtained using an Avance DPX-500 NMR spectrometer (Bruker, USA) at 35 and 60 °C with methanol as the internal standard. The sample concentration was 15 mg of polysaccharide/mL of D_2O.

2.2. Preparation of silver nanoparticles (Ag-NPs)

Ten mg of each polysaccharide – alginate, fucoidan, laminaran – were directly dissolved in 100 mL of 1 mM $AgNO_3$ aqueous solution with stirring at room temperature. The pH of the obtained solutions was adjusted to 10–11 by KOH. After that, the reaction mixture was kept on a magnetic stirrer for 30 min under constant heating (70 °C). The reduction of Ag^+ ions to silver nanoparticles was monitored by visual inspection of the color change in solution and was apparent immediately after the beginning of the reaction. Particles synthesized with ScL, ScF, FeF and FeA were designated Ag-NPs-ScL, Ag-NPs-ScF, Ag-NPs-FeF, and Ag-NPs-FeA, respectively. The nanoparticles were repeatedly centrifuged at 20,000x*g* for 30 min (5430R, Eppendorf) and washed with sterile Milli-Q® water before further analysis. Aliquots (1 mL) of each sample were dried under vacuum and weighted using the analytical electrical balance to determine the concentration of the reduced Ag° crystals.

2.3. Characterization of the NPs

2.3.1. UV–vis spectrophotometric analysis

The color change of the reaction medium was monitored initially by periodic sampling of reaction solutions and then by measuring UV–vis absorption. The aliquots of reaction mixtures (2 μL) were analyzed by Biospec-nano spectrophotometer (Shimadzu, Japan) in the range of 200–800 nm. Silver nitrate (1 mM) was used for the baseline correction.

2.3.2. Fourier transform infrared spectroscopy analysis

Fourier transform infrared spectroscopy (FTIR) analysis were done with Shimadzu FTIR-8400 spectrometer at room temperature over the range of $4000-400\ cm^{-1}$ at a resolution of $3\ cm^{-1}$ in KBr pellets.

2.3.3. Nanoparticle tracking analysis

Hydrodynamic diameter and Z-potential of the nanoparticles were measured by nanoparticle tracking analysis (NTA) using a Nanosight NS500 system (NanoSight, UK) following the manufacturer's instructions. Samples were diluted with water to obtain approximately 20 particles per image before analysis. The measurements were made at room temperature and 60 s capture of particle movement under Brownian motion. The captured videos (10 videos per sample) were processed and analyzed by NTA analytical software version 2.2. The script for video recording and the manufacturer designed analysis was employed to estimate Z-potential.

2.3.4. Transmission electron microscopic (TEM) analysis

TEM images were obtained by Libra 200 (Carl Zeiss, Germany) microscope. Samples were dispersed in ethanol using the ultrasound bath IC1216-40-12 (Branson, USA) (ultrasonic dispersing mode: duration 3 h, 25 °C). Droplets of this dispersion were placed onto a carbon-coated copper grids 3250C (SPI, USA) for imaging.

2.3.5. X-ray diffraction studies

The crystalline nature of the impregnated Ag-NPs was investigated using an X-ray diffraction (XRD) analysis. The XRD pattern was recorded using Miniflex II (Rigaku, Japan) operated at 30 kV with a current of 15 mA and Cu/Ka radiation in the range of 3°–80° in 2θ angles. Results were compared with the standard powder diffraction card no. 04-0783 of Joint Committee on Powder Diffraction Standards. The average particle size of the synthesized Ag-NPs was calculated using the Scherrer equation:

$$D = 0.94\ \lambda / \beta\ Cos\theta,$$

where λ is the X-ray wavelength (1.5418 Å), β is the full width at half maximum (FWHM) and θ is the diffraction angle.

2.3.6. Cell culture and Ag-NPs treatment

C6 (rat glioma) cells were cultured in DMEM media (Gibco®, USA) supplemented with 10 % fetal bovine serum (Gibco®, USA) and 1 % Antibiotic-Antimycotic (Gibco®, USA) that contains penicillin, streptomycin and amphotericin B, in 25 cm^2 flasks (Eppendorf, Germany) incubated at 37 °C in a 5 % carbon dioxide humidified incubator until 80 % confluence. Cells were washed with PBS (0.8 % NaCl. 0.02 % KCl. 10 mM Na_2HPO_4-KH_2PO_4, pH 7.4) and trypsinized with 0.25 % trypsin (Gibco®, USA). After harvest, C6 was seeded in two 96-well plates with 0.7×10^4 cells per well and four 24-well plates with the concentration of 2.8×10^4 cells per well. Cells were counted by MoFlo Astrios EQ sorter (Beckman Coulter, USA). After 24 h incubation to allow cell attachment, different concentrations of Ag-NPs-FeF, Ag-NPs-FeA, Ag-NPs-

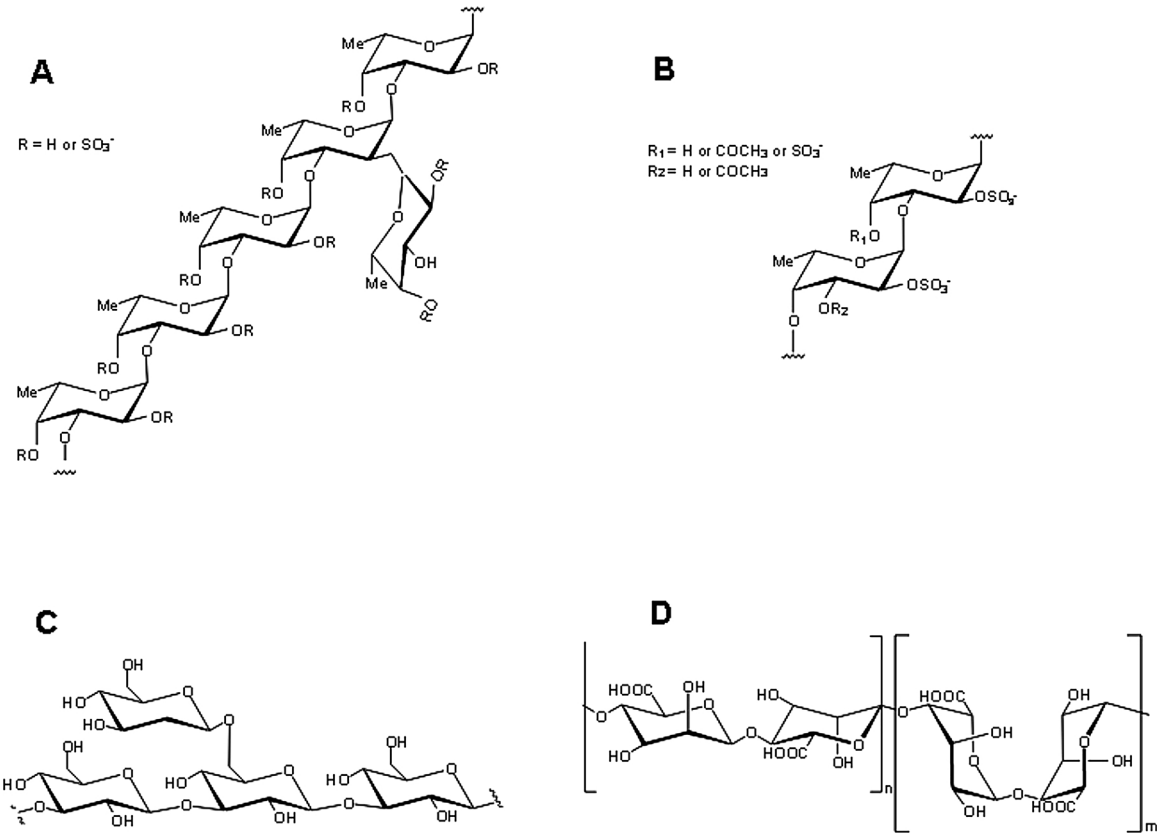

Fig. 1. The main structural fragments of ScF (A), ScL (B), FeF (C) and FeA (D).

ScF, and Ag-NPs-ScL (1, 5, 12.5, 25, 50 and 100 μg/mL) were added to 96-well plates for 24 h, to survey their cytotoxicity. Equivalent concentrations of Ag-NPs were added to 24-well plates to track proliferation activity; these samples were analyzed immediately.

2.3.7. MTT assay

After incubation with different types of Ag-NPs 10 μL of MTT solution (0.5 mg/mL) per well was added to the 100 μL of the culture medium for 4 h at 37 °C. Then, the solution was discarded, 150 μL of lysis buffer (4 mM HCl with isopropanol, 1 % NP-40) was added to the cells to dissolve the formed formazan crystals, and the lysates were incubated 30 min at room temperature. Afterwards, the plates were centrifuged for 10 min at 1000*g* (Eppendorf® Centrifuge 5804-R, Germany), and 100 μL of supernatant from each sample was added to the new well. The absorbance was measured with the absorbance microplate reader (iMark™, Bio Rad, USA) at 595 nm with 655 nm. The difference in values obtained at 655 nm and 595 nm was estimated as absorbance of nanoparticles cytotoxicity effects.

2.3.8. High-content imaging analysis

High-throughput imaging with Cell-iQ® platform (Chip-Man Technologies Ltd, Finland) was used to track proliferation activity. C6 cells seeded in 24-well plates at density 2.8 × 10^4 cells per well and treated by 1, 5, 12.5, 25, 50 and 100 μg/mL of Ag-NPs were incubated in 5 % CO_2, 37 °C and monitored for 44 h until controls formed the monolayer to analyze cell growth. Results are presented as the proliferation index, calculated as the sum of cells in all generations divided by the number of the initially seeded cells.

2.3.9. Antibacterial activity

Antibacterial activity of synthesized Ag-NPs against two gram-negative bacteria *Escherichia coli* and *Agrobacterium tumefaciens* was evaluated by the disk-diffusion method. Bacterial strains were freshly cultivated for 24 h at 37 °C (*E. coli)* or 28 °C (*A. tumefaciens)* in Luria-Bertani (LB) broth. Each bacterial culture containing 1 × 10^6 CFU/mL was spread on the LB agar plates. Sterile paper discs (diameter 5 mm) containing four different concentrations of Ag-NPs (5, 10, 15, 20 μg/disk) were placed and incubated at an appropriate temperature for 24 h. Following incubation, the zone free of the bacterial cells (i.e. the zone of inhibition) from edge to edge of the cleared area was measured with a ruler. Experiments were done in triplicate.

3. Results and discussion

3.1. Isolation and characterization of individual polysaccharides from brown algae F. evanescens and S. cichorioides

The highly purified fractions of alginate (FeA) and fucoidan (FeF) were obtained from *F. evanescens*; laminaran (ScL) and fucoidan (ScF) – from *S. cichorioides*; structural characteristics of obtained polysaccharides were determined using spectroscopy NMR.

NMR spectra of FeA were specific for algal alginates and contained intensive signals, corresponding to 1.4-linked residues of β-D-mannuronic acid and less intense peaks for 1.4-linked residues of α-L-guluronic acids. The yield of FeA was 18 % of dry defatted alga weight.

Both fucoidans were sulfated fucans, differing by types of bonds between fucose residues (1.3- and 1.4- for FeF; 1.3- for ScF) and sulfate degrees (27 % for FeF and 36 % for ScF). Fucoidan FeF also contained acetyl groups that ScL did not have. Earlier, the structures of these polysaccharides were established (Menshova et al., 2016; Zvyagintseva et al., 2003). The NMR spectra of the polysaccharides obtained in present work were the same as those previously isolated. So, FeF was weakly-branched fucan, containing alternating 1.3- and 1.4-linked fucopyranose residues in the main chain. Sulfate groups were found mainly at position 2 and less at 4 (Menshova et al., 2016). Fucan ScF had the main chain predominantly with 1.3-linked fucopyranose

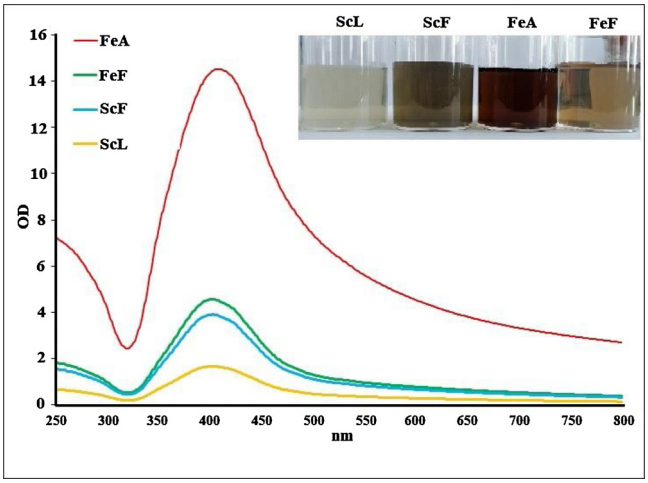

Fig. 2. UV–vis spectra of silver nanoparticles prepared at 70 °C, pH 10 and 0.1 mg/mL of alginate (FeA) and fucoidan (FeF) from *F. evanescenes*, fucoidan (ScF) and laminaran (ScL) from *S. cicharioides*. Inset image represents the corresponding Ag-NPs colloids.

residues and less of 1.4-linked residues and branches in the form of single fucose residues at C2. Sulfates were in positions 2 and 4 (Zvyagintseva et al., 2003).

According to spectroscopy NMR, the laminaran ScL was 1.3;1.6-β-D-glucan with the ratio of bonds 1.3:1.6 = 9:1. This polysaccharide contained the main chain from 1.3-linked glucose residues with single branches at C6 (Malyarenko et al., 2017). The main structural fragments of all obtained polysaccharides are shown in Fig. 1.

Thus, from brown algae *F. evanescens* and *S. cichorioides,* we obtained individual highly purified fractions of three types of polysaccharides with known structural characteristics.

3.2. Synthesis of silver nanoparticles

When the samples of different seaweed polysaccharides were added to silver nitrate solution, pH adjusted and heated, the color of the reaction began immediately turn from colorless to brownish. The intensity of the brown color increased rapidly, from seconds to a few minutes for different types of polysaccharides and then stayed stable within an hour of observation. It is well known that Ag-NPs colloids have brown coloration due to their characteristic excitation of surface plasmons in the range of 400–490 nm (Gilaki, 2010). Therefore, a transition of the solution from colourless to brown indicates the formation of Ag-NPs (Vanaja et al., 2013). Similarly, fucoidan from *Turbinaria conoides* catalyzed the formation of Ag-NPs within 15 min of reaction (Kala, Prashob Peter, & Chandramohanakumar, 2016). However, when fucoidan from *Fucus vesiculosus* was used for silver ion reduction, characteristic surface plasmon resonance peak was observed after 2 h of reaction only, and the intensity increased with time and completed after a day (Venkatesan, Singh, Anil, Kim, & Shim, 2018). This result means that different polysaccharides have different silver ions reduction rates.

The UV–vis spectra of the synthesized Ag-NPs-FeA, Ag-NPs-FeF, Ag-NPs-ScF, and Ag-NPs-ScL demonstrated the maximum peaks at 408, 402, 412 and 414 nm, respectively, as shown in Fig. 2. Similar surface plasmon resonance (SPR) peaks were observed in many studies of green synthesis for silver nanoparticles. For example, onion (*Allium cepa*)

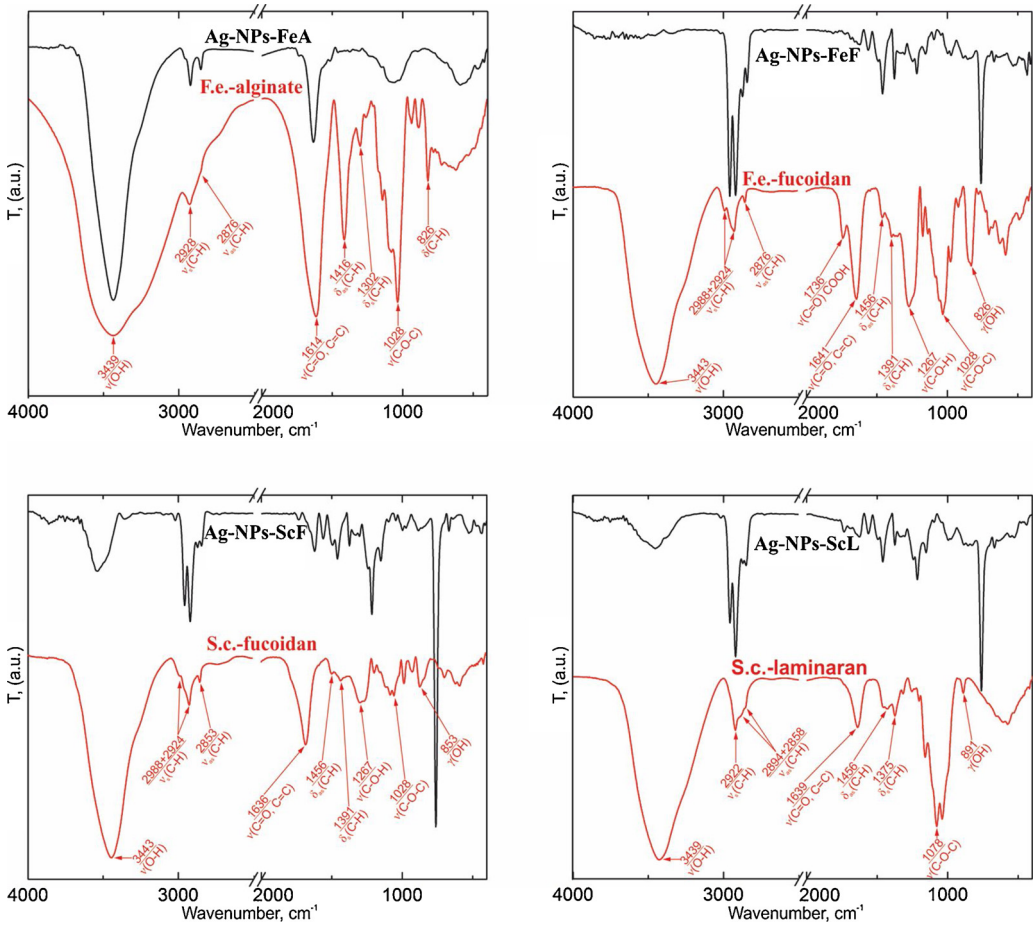

Fig. 3. FTIR spectra obtained from silver nanoparticles: (A) – Ag-NPs-FeA and FeA, (B) – Ag-NPs-FeF and FeF, (C) – Ag-NPs-ScF and ScF, (D) – Ag-NPs-ScL and ScL.

Table 1
Assignment of FTIR spectra of polysaccharides and their complexes with Ag-NPs.

Samples / IR-bands description	ν(OH, NH)	ν_s(CH)	ν_{as}(CH)	ν(C = O, C = C)	δ_{as}(CH)	δ_s(CH)	ν(C-O-C)	δ(CH)
Ag-NPs-FeA	3437	2920	2853	1636	1460	1377	1063	–
FeA	3439	2928	2876	1614	1416	1302	1028	826
Ag-NPs-FeF	3440	2918	2841	1619	1460	1377	1006	–
FeF	3443	2924	2853	1641	1456	1391	1028	826
Ag-NPs-ScF	3537	2920	2841	1620	1460	1377	1006	–
ScF	3443	2924	2853	1636	1456	1391	1028	826
Ag-NPs-ScL	3452	2920	2851	1636	1460	1377	995	887
ScL	3429	2922	2858	1639	1456	1375	1040	891

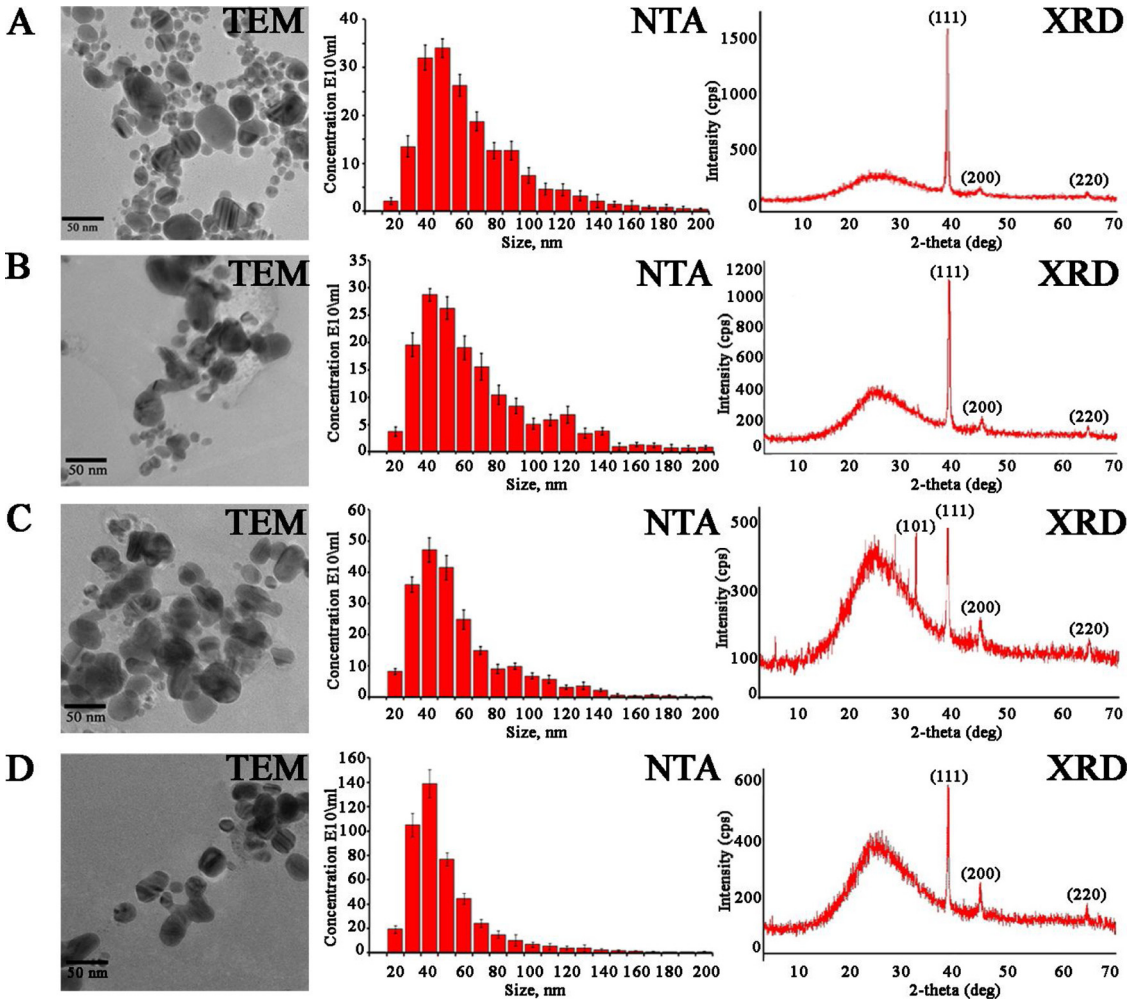

Fig. 4. Ag-NPs obtained using alginate from *F. evanescens* (A), fucoidan from *F. evanescens* (B), fucoidan from *S. cichorioides* (C), laminaran from *S. cichorioides* (D). TEM – images of transmission microscopy; NTA – nanoparticle tracking analysis of Ag-NPs size distribution; XRD – X-ray diffraction spectra of Ag-NPs.

extract promoted Ag-NPs with SPR peak at 413 nm (Balamanikandan, Balaji, & Pandiarajan, 2015). Similarly, cellulose powder, microcrystalline cellulose, carboxymethyl cellulose, and chitosan were used to obtain nanosilver with peaks at 407, 402, 403 and 405 nm, respectively (Hassabo, Nada, Ibrahim, & Abou-Zeid, 2015). Notably, in the same reaction conditions, the optical density of Ag-NPs-FeA was 3.18, 3.72, and 8.75 times higher than that of Ag-NPs-FeF, Ag-NPs-ScF, and Ag-NPs-ScL, respectively. At the same time, the reduction properties of fucoidans from *F. evanescenes* and from *S. cichorioides* were almost the same. They exceeded the reduction strength of laminaran from *S. cichorioides* by 2.74 and 2.35, respectively. Therefore, our data suggest that fucoidan and laminaran have less reduction potential than alginate. Finally, based on the spectrum data, we can conclude that the reduction properties of polysaccharides increase in the following order: ScL, ScF, FeF, and FeA.

3.3. Characterization of silver nanoparticles

The FTIR analysis was performed to confirm the involvement of polysaccharides in Ag-NPs biosynthesis. Fig. 3 shows the FTIR spectra obtained from all investigated silver nanoparticles as well as that measured from initial polysaccharides. Polysaccharides FeA, FeF, ScF and ScL showed several characteristic peaks (Table 1): the peaks at 3439, 3443, 3443, 3429 cm^{-1} is due to (OH) and (NH−−) stretching vibrations, respectively; symmetric and asymmetric (C−H) stretching vibrations satisfy 2922–2928 and 2853 − 2876 cm^{-1}, respectively; vibrations of (C═O) and (CC═) groups ranged from 1614 to 1641 cm^{-1}; bending vibrations of methyl and methylene groups are visible at

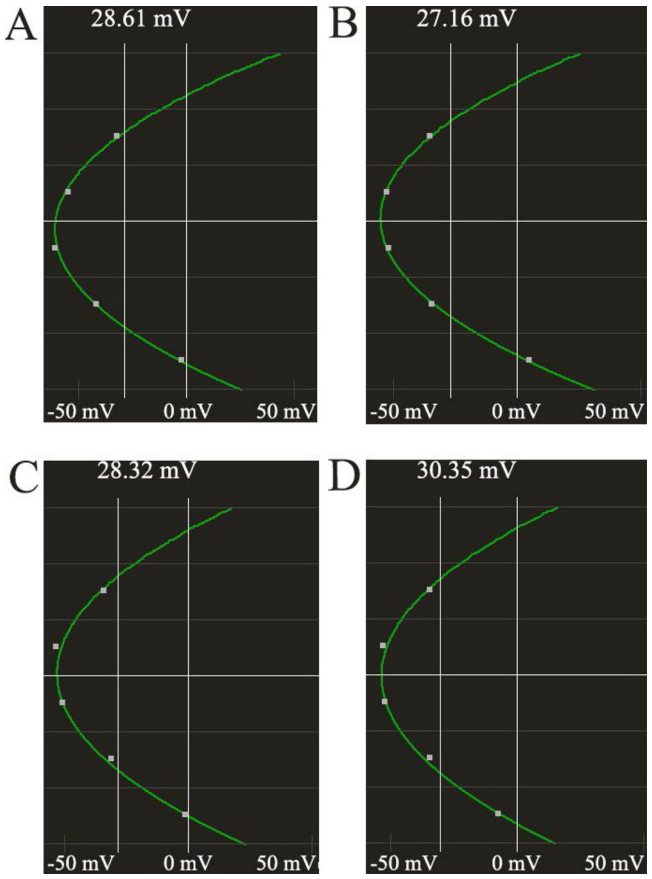

Fig. 5. Mobility curve corrected for cell flow (on completion, curve mean is zeta-potential). Ag-NPs obtained using alginate from *F. evanescens* (A), fucoidan from *F. evanescens* (B), fucoidan from *S. cichorioides* (C), laminaran from *S. cichorioides* (D).

1416–1456 and 1302 − 1391 cm^{-1}, respectively; 1028 − 1040 cm^{-1} can be attributed to the stretching vibration of (C—OC) bond; 826 − 891 $c--^{-1}$ is due to the deformation vibrations in CH2. Skeletal deformation bands occur in the region 700 − 500 cm^{-1}. Thus, our data demonstrate that FTIR bands are attributed to the vibration of functional groups of polysaccharide (Socrates, 2004). The bands attributed to initial polysaccharides were also observed in the spectra of synthesized Ag-NPs samples (Fig. 3, Table 1). It may means that the polysaccharides act as a bioreductants and stabilizers. Similar FTIR spectra for polysaccharide-catalyzed nanoparticles were obtained for green alga extract from *Botryococcus braunii* (Arya, Gupta, Chundawat, & Vaya, 2018) and for polysaccharide extract from cactus pads (Onditi, Bosire, Changamu, & Ngila., 2019).

Fig. 4 shows the size distribution and morphology of Ag-NPs prepared using different polysaccharides. The transmission electron microscopy (TEM) images of Ag-NPs-FeA, Ag-NPs-FeF, Ag-NPs-ScF, Ag-NPs-ScL shows the prevalence of spherical shaped particles with average sizes of 57 ± 9, 64 ± 6, 53 ± 4, 45 ± 2 nm, respectively. This result is in accordance with the data obtained by NTA measurements of corresponding particle size distributions shown in Fig. 4 (NTA). Z-potential for all Ag-NPs was found to be in the range −27 to −30 mV (Fig. 5). Similar spherical Ag-NPs with the size of 50 nm and highly negative Z-potential up to −36 mV were previously obtained with chitosan and fucoidan (Venkatesan et al., 2018).

X-ray diffraction (XRD) spectra were recorded to verify the crystallinity of obtained polysaccharide-based nanoparticles (Fig. 3 XRD). The peaks of Ag-NPs-FeA, Ag-NPs-FeF, Ag-NPs-ScL in the entire spectrum of 2θ values were assigned to (111), (200), (220) Bragg reflection of a face-centred cubic (fcc) Ag metallic structure (Ashokkumar et al., 2015). Ag-NPs-ScF had an additional 2θ value assigned to (101) Bragg reflection. These results are in agreement with the data for the biosynthesis of Ag-NPs with konjac glucomannan, carrageenan and inulin (Zhang et al., 2018) and sulfated polysaccharide from *Porphyravietnamensis* (Venkatpurwar & Pokharkar, 2011). The average crystalline size of Ag-NPs-FeA, Ag-NPs-FeF, Ag-NPs-ScF, Ag-NPs-ScL was calculated using the Scherrer formula and found to be about 18, 24, 37, 29 nm, respectively. The much smaller sizes of Ag-NPs evaluated with the use of XRD comparative to NTA or TEM are not surprising and could be associated with the not ideal spherical shape of particles, a polycrystalline structure, impurities or variation in their hydrodynamic diameter (Shkryl et al., 2018).

3.4. Proliferation and viability of rat glioma cell line (C6) treated by Ag-NPs

The cytotoxicity of Ag-NPs-FeA, Ag-NPs-FeF, Ag-NPs-ScF, Ag-NPs-ScL against rat glioma cell line (C6) was studied by MTT assay and results are shown in Fig. 6. The Ag-NPs-FeA and Ag-NPs-ScL demonstrated substantial cytotoxic effect in a dose-dependent manner. In case of Ag-NPs-FeA, the maximal cytotoxicity was achieved at a dose of 50 μg/mL, while Ag-NPs-ScL demonstrated high cytotoxicity effect at 25 μg/mL. At the same time, the toxicity of Ag-NPs-FeF and Ag-NPs-ScF on C6 cells was less pronounced. In particular, Ag-NPs-FeF at 50 μg/mL inhibited cell viability by only 1.2 times but completely abolished growth at 100 μg/mL. Interestingly, under our conditions, Ag-NPs-ScF possessed the highest cytotoxicity threshold among the four tested polysaccharides, i.e. C6 cells demonstrated excellent viability up to 100 μg/mL and a dose-dependent cytotoxicity, yet much less significant than other Ag-NPs samples. Also, the dynamic of C6 growth in the presence of Ag-NPs was measured with the Cell-iQ® assay (Fig. 7). According to obtained data, 12.5 μg/mL of Ag-NPs-ScL was enough to inhibit proliferation index of C6 cells by more than 2-fold. At the same time, a further increase in concentration completely prevented biomass accumulation during the whole span of observation. Ag-NPs-FeF and Ag-NPs-FeA proved to possess intermediate cytotoxicity as their maximal effect was evident only at 100 μg/mL. Ag-NPs-ScF seems to be less effective in case of rat glioma because C6 cells were viable at all tested concentrations of nanoparticles.

Similar cytotoxicity of Ag-NPs biosynthesized with *Beta vulgaris* was observed against MCF7, A549, and Hep2 cell lines (Venugopal et al., 2017). Silver nanoparticles may also suppress the viability of normal human skin fibroblast cell line (HSF-PI-16) with an IC_{50} value of 30.64 μg/mL (Paknejadi, Bayat, Salimi, & Razavilar, 2018). However, Ag-NPs prepared using a fibrinolytic enzyme from *Bacillus cereus* did not have significant toxicity on the murine RAW 264.7 macrophage cell line in concentrations up to 100 μg/mL (Deepak et al., 2011).

It is known that the all polysaccharide from brown algae are almost non-toxic (Malyarenko & Ermakova, 2017); previously used polymers are no exception (Malyarenko et al., 2017; Menshova et al., 2016; Usoltseva et al., 2019), while the investigated nanoparticles exhibit varying degrees of cytotoxicity. Thus, our data clearly indicate, that the cytotoxicity of nanoparticles varies depending on the properties of polymer matrixes.

3.5. Determination of the antibacterial activity

We also studied the antimicrobial activity of polysaccharide-based silver nanoparticles against gram-negative bacteria *Escherichia coli* and *Agrobacterium tumefaciens* using an agar disk-diffusion method. The clear zone around the disk with nanoparticles suggests that they possess antibacterial activity, which can inhibit the growth of pathogens (Guzman, Dille, & Godet, 2012). After incubation of *E. coli* and *A. tumefaciens* with different concentrations of Ag-NPs, we observed that all tested nanoparticles significantly inhibited the growth of both bacteria in a concentration-dependent manner (Fig. 8). No inhibition was

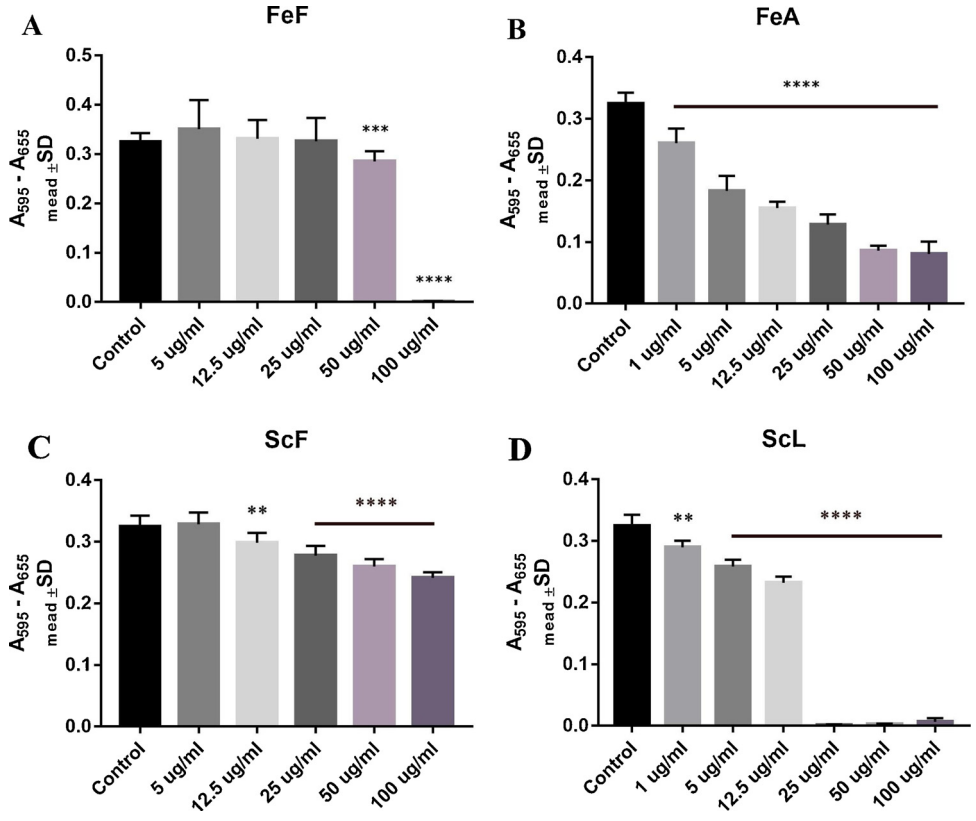

Fig. 6. MTT assay and cell proliferation rates of rat glioma cells C6. C6 cells were treated with Ag-NPs synthesized using FeF (A), FeA (B), ScF (C) and ScL (D) in 1, 5, 12.5, 25, 50 and 100 μg/mL concentrations. Data are presented as the mean ± SE, **p < 0.01, ***p < 0.001, **** p < 0.0001.

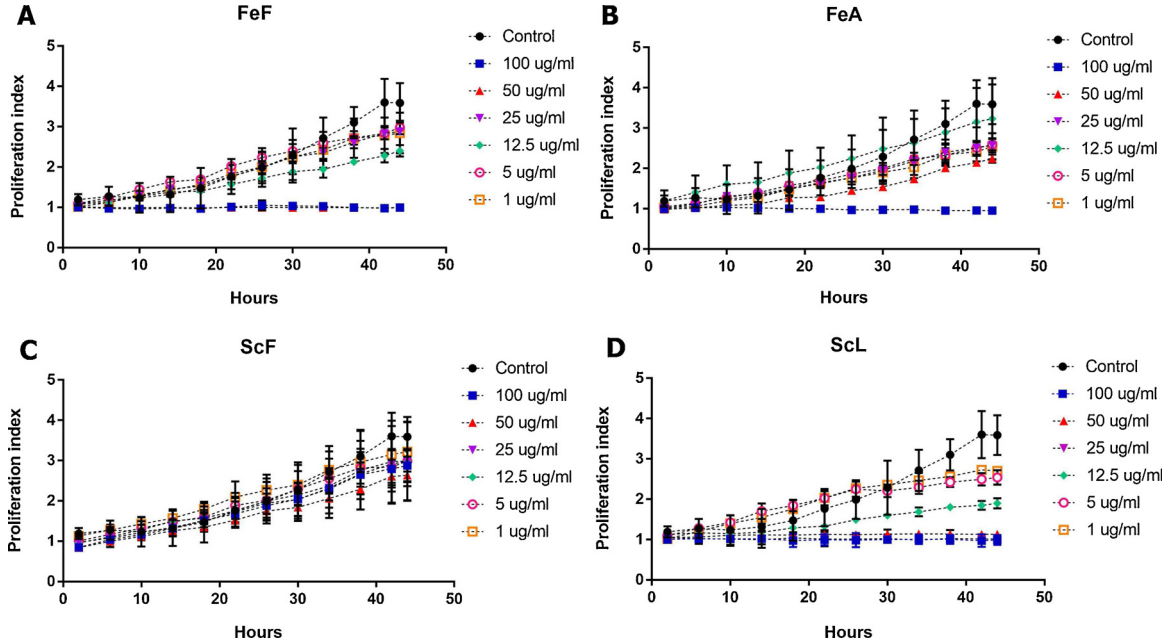

Fig. 7. Growth curves of rat glioma cells C6 measured with the Cell-iQ® assay. C6 cells were treated with Ag-NPs synthesized using FeF (A), FeA (B), ScF (C) and ScL (D) in 1, 5, 12.5, 25, 50 and 100 μg/mL concentrations and monitored for 44 h. Data are presented as the mean ± SE.

detected when using the negative control – i.e. aqueous solutions of each polysaccharide. It was shown previously that chitosan-fucoidan complex-coated Ag-NPs demonstrated maximal biocidal action against gram-negative *E. coli* at a concentration of 10 μg/disk with the zone of inhibition reaching 3.0 ± 0.3 mm (Venkatesan et al., 2018). Similarly, our samples of Ag-NPs-FeA, Ag-NPs-FeF, Ag-NPs-ScF, Ag-NPs-ScL demonstrated 3.5, 3, 1.5, 3 mm zone of *E. coli* growth inhibition, respectively, when applied at 10 μg/disk. Previously, biocidal activities against *E. coli* was demonstrated for Ag-NPs synthesized using green alga *Botryococcus braunii* (Arya et al., 2018), polysaccharide extract from cactus pads (Onditi et al., 2019), and polysaccharides isolated from red marine algae (de Aragao et al., 2019).

Suppression of *A. tumefaciens* growth by polysaccharide-based AgNPs was generally more pronounced than that for *E. coli*(Fig. 8).

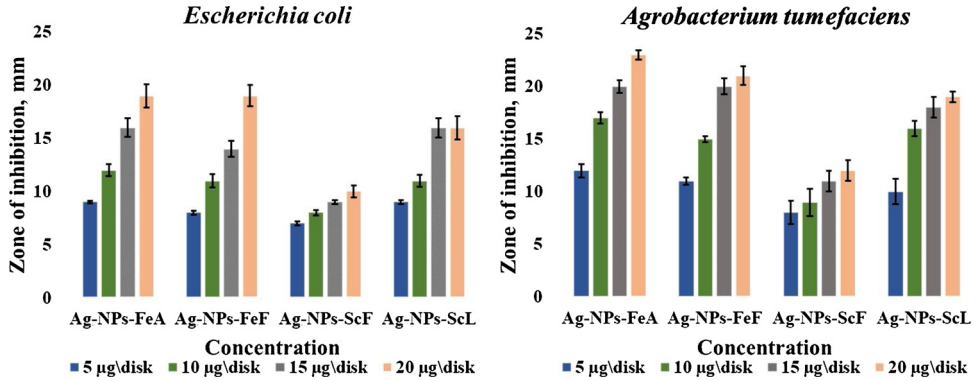

Fig. 8. Inhibition zone diameter (mm) of Ag-NPs obtained with different polysaccharides against *E. coli* and *A. tumefaciens*. Data are presented as the mean ± SE.

Thus, Ag-NPs-FeA increased inhibition zone by 1.42 times, Ag-NPs-FeF – by 1.36 times, Ag-NPs-ScF – by 1.13 times and Ag-NPs-ScL – by 1.45 times. In our previous work, silver nanoparticles obtained using silicatein-expressing transgenic tobacco callus extract also showed a more pronounced antibacterial effect against *A. tumefaciens* than against *E. coli* (Shkryl et al., 2018). The difference in the antibacterial effectiveness of nanoparticles against various pathogens may depend on many factors, and the exact mechanisms of Ag-NPs action remain unknown. However, some researchers propose that pronounced activity of nanosilver may be related with its ability for electrostatic interaction with the bacterial cell wall (Hamouda & Baker, 2000; Shrivastava et al., 2007). Ag-NPs also provoke the formation of free radicals (Danilczuk, Lund, Sadlo, Yamada, & Michalika, 2006; Dakal, Kumar, Majumdar, & Yadav, 2016), leading to DNA damage and protein inactivation (Rai, Deshmukh, Ingle, & Gade., 2012). It was reported that Ag-NPs could change the membrane morphology and alter the membrane permeability, thus affecting cell signaling (Sondi & Salopek-Sondi, 2004). Usually, the toxicity of silver nanoparticles against gram-positive bacteria is higher than against gram-negative bacteria, and this phenomenon can be related to the differences in chemical nature and depth of their cell walls (Kala et al., 2016; Son, Youk, & Park, 2006). It was shown that a much higher concentration of Ag-NPs is required to destroy *Staphylococcus aureus* cells compared to commonly used *E. coli* (Feng et al., 2000). Also, size and shape of Ag-NPs are known to contribute significantly to their antibacterial effects (Martinez-Castanon, Nino-Martinez, Martinez-Gutierrez, Martinez-Mendoza, & Ruiz, 2008; Meire, Coenye, Nelis, & De Moor, 2012; Pal, Tak, & Song, 2007) (Fig. 8).

4. Conclusion

The present study provides an alternative eco-friendly synthesis of monodispersed and spherical shaped Ag-NPs using three different types (alginate, fucoidan, laminaran) of algal polysaccharides. We investigated nanoparticle formation by UV–vis assay, and the crystalline structure of formed polysaccharide-based Ag-NPs was confirmed by XRD patterns. The TEM images demonstrated that the average size of obtained Ag-NPs was about 54 nm and that they were predominantly spherical. NTA analysis confirmed the size distribution of Ag-NPs and showed their highly negative Z-potential, potentially indicating the electrostatic stability of obtained nanosilver. The FTIR spectra confirmed that polysaccharides were responsible for the reduction of silver nitrate to Ag-NPs and also acted as stabilizing agents. The Ag-NPs-FeA and Ag-NPs-ScL showed pronounced cytotoxicity toward rat glioma cells. The prepared metal nanoparticles had antibacterial activity against plant and animal pathogens such as *A. tumefaciens* and *E. coli*. Thus, polysaccharide-stabilized metal nanoparticles can be further investigated for their potential in various nanotechnology-based biomedical applications and can potentially reduce the destructive effects associated with the traditional methods for nanoparticles synthesis.

CRediT authorship contribution statement

Y.A. Yugay: Conceptualization, Investigation, Formal analysis, Visualization, Writing - original draft. **R.V. Usoltseva:** Resources, Formal analysis, Validation, Visualization, Writing - review & editing. **V.E. Silant'ev:** Investigation, Formal analysis, Validation, Visualization, Writing - review & editing. **A.E. Egorova:** Investigation, Formal analysis, Validation, Visualization, Writing - review & editing. **A.A. Karabtsov:** Investigation, Formal analysis, Validation, Writing - review & editing. **V.V. Kumeiko:** Resources, Supervision, Writing - review & editing. **S.P. Ermakova:** Resources, Supervision, Writing - review & editing. **V.P. Bulgakov:** Resources, Supervision, Writing - review & editing. **Y.N. Shkryl:** Conceptualization, Methodology, Validation, Supervision, Writing - review & editing.

Acknowledgment

The investigations were conducted using equipment from the Instrumental Centre for Biotechnology and Gene Engineering at the Federal Scientific Centre of the East Asia Terrestrial Biodiversity of the Far Eastern Branch of the Russian Academy of Sciences (Vladivostok). XRD analysis was performed at the Centre for Elemental and Isotopic Analysis at the Far Eastern Geological Institute of the Far Eastern Branch of Russian Academy of Science (Vladivostok). TEM images were obtained at the Far Eastern Center for Electron Microscopy at the A.V. Zhirmunsky National Scientific Center of Marine Biology of the Far Eastern Branch of the Russian Academy of Sciences (Vladivostok). The reported study was funded by RFBR: isolation and characterization of polysaccharides by Grant No. 18-04-00905; synthesis, characterization and biological activities of silver nanoparticles by Grant No. 19-34-90184. Antibacterial activity evaluation was funded by a grant from the Far Eastern Branch of the Russian Academy of Sciences No. 18-4-051.

References

Amkamwar, B., Damle, C., Ahmad, A., & Sastry, M. (2005). Biosynthesis of gold and silver nanoparticles using *Emblica officinalis* fruit extract, their phase transfer and transmetallation in an organic solution. *Journal of Nanoscience and Nanotechnology, 5*, 1665–1671.

Aramwit, P., Bang, N., Ratanavaraporn, J., & Ekgasit, J. S. (2014). Green synthesis of silk sericin-capped silver nanoparticles and their potent anti-bacterial activity. *Nanoscale Research Letters, 9*, 79.

Arya, A., Gupta, K., Chundawat, T. S., & Vaya, D. (2018). Biogenic synthesis of copper and silver nanoparticles using green alga *Botryococcus braunii* and its antimicrobial activity. *Bioinorganic Chemistry and Applications, 2018*, 7879403.

Balaji, D. S., Basavaraja, S., Bedre, M. D., Prabhakar, B. K., & Venkataraman, A. (2011). Biosynthesis of silver nanoparticles by fungus *Trichoderma reesei*. *Insciences Journal, 1*, 65–79.

Balamanikandan, T., Balaji, S., & Pandiarajan, J. (2015). Biological synthesis of silver nanoparticles by using onion (*Allium cepa*) extract and their antibacterial and antifungal activity. *World Applied Sciences Journal, 33*, 939–943.

Bhainsa, K. S., & D'Souza, S. F. (2006). Extracellular biosynthesis of silver nanoparticles using the fungus *Aspergillus fumigates*. *Colloids and Surfaces B, Biointerfaces, 47*, 160–164.
Chandran, S. P., Chaudhary, M., Pasricha, R., Ahmad, A., & Sastry, M. (2006). Synthesis of gold nanotriangles and silver nanoparticles using *Aloe vera* plant extract. *Biotechnology Progress, 22*, 577–583.
Chumpol, J., & Siri, S. (2018). Simple green production of silver nanoparticles facilitated by bacterial genomic DNA and their antibacterial activity. *Artificial Cells, Nanomedicine, and Biotechnology, 46*, 619–625.
Dakal, T. C., Kumar, A., Majumdar, R. S., & Yadav, V. (2016). Mechanistic basis of antimicrobial actions of silver nanoparticles. *Frontiers in Microbiology, 7*, 1831.
Danilczuk, M., Lund, A., Sadlo, J., Yamada, H., & Michalika, J. (2006). Conduction electron spin resonance of small silver particles. *Spectrochimica Acta Part A, Molecular and Biomolecular Spectroscopy, 63*, 189–191.
de Aragao, A. P., de Oliveira, T. M., Quelemes, P. V., Perfeito, M. L. G., Araujo, M. C., Santiago, J. D. S., et al. (2019). Green synthesis of silver nanoparticles using the seaweed *Gracilaria birdiae* and their antibacterial activity. *Arabian Journal of Chemistry, 12*, 4182–4188.
Deepak, V., Umamaheshwaran, P. S., Guhan, K., Nanthini, R. A., Krithiga, B., Jaithoon, N. M. H., et al. (2011). Synthesis of gold and silver nanoparticles using purified URAK. *Colloids and Surfaces B, Biointerfaces, 86*, 353–358.
Dodgson, K. S. (1961). Determination of inorganic sulphate in studies on the enzymic and non-enzymic hydrolysis of carbohydrate and other sulphate esters. *The Biochemical Journal, 78*, 312–319.
Dubois, M., Gilles, K. A., Hamilton, J. K., Rebers, P. A., & Smith, F. (1956). Colorimetric method for determination of sugars and related substances. *Analitical Chemistry, 28*, 350–356.
El-Rafie, H. M., El-Rafie, M. H., & Zahran, M. K. (2013). Green synthesis of silver nanoparticles using polysaccharides extracted from marine macro algae. *Carbohydrate Polymers, 96*, 403–410.
Feng, Q. L., Wu, J., Chen, G. Q., Cui, F. Z., Kim, T. N., & Kim, J. O. (2000). A mechanistic study of the antibacterial effect of silver ions on *Escherichia coli* and *Staphylococcus aureus*. *Journal of Biomedical Materials Research, 52*, 662–668.
Gao, Y., & Cranston, R. (2008). Recent advances in antimicrobial treatments of textiles. *Textile Research Journal, 78*, 68–72.
Garza-Navarro, M. A., Aguirre-Rosales, J. A., Llanas-Vázquez, E. E., Moreno-Cortez, I. E., Torres-Castro, A., & González-González, V. (2013). Totally ecofriendly synthesis of silver nanoparticles from aqueous dissolutions of polysaccharides. *International Journal of Polymer Science, 2013*, 436021.
Gilaki, M. (2010). Biosynthesis of silver nanoparticles using plant extracts. *The Journal of Biological Sciences, 10*, 465–467.
Gour, A., & Jain, N. (2019). Advances in green synthesis of nanoparticles. *Artificial Cells, Nanomedicine, and Biotechnology, 47*, 844–851.
Gunti, L., Dass, R. S., & Kalagatur, N. K. (2019). Phytofabrication of selenium nanoparticles from*Emblica officinalis* fruit extract and exploring its biopotential applications: antioxidant, antimicrobial, and biocompatibility. *Frontiers in Microbiology, 10*, 931.
Guzman, M., Dille, J., & Godet, S. (2012). Synthesis and antibacterial activity of silver nanoparticles against gram-positive and gram-negative bacteria. *Nanomedicine, 8*, 37–45.
Hamouda, T., & Baker, J. R. (2000). Antimicrobial mechanism of action of surfactant lipid preparations in enteric gram-negative bacilli. *Journal of Applied Microbiology, 89*, 397–403.
Hassabo, A. G., Nada, A. A., Ibrahim, H. M., & Abou-Zeid, N. Y. (2015). Impregnation of silver nanoparticles into polysaccharide substrates and their properties. *Carbohydrate Polymers, 122*, 343–350.
Huang, H., & Yang, X. (2004). Synthesis of polysaccharide-stabilized gold and silver nanoparticles: A green method. *Carbohydrate Research, 339*, 2627–2631.
Kala, K. J., Prashob Peter, K. J., & Chandramohanakumar, N. (2016). Analysis of antimicrobial potential of silver nanoparticles synthesized by fucoidan isolated from *Turbinaria conoides*. *International Journal of Pharmacognosy and Phytochemical Research, 8*, 1959–1963.
Kowshik, M., Ashtaputre, S., Kharrazi, S., Vogel, W., Urban, J., Kulkarni, S. K., et al. (2002). Extracellular synthesis of silver nanoparticles by a silver-tolerant yeast strain MKY3. *Nanotechnology, 144*, 95–100.
Kumar, S. A., Abyaneh, M. K., Gosavi, S. W., Kulkarni, S. K., Pasricha, R., Ahmad, A., et al. (2007). Nitrate reductase-mediated synthesis of silver nanoparticles from $AgNO_3$. *Biotechnology Letters, 29*, 439–445.
Lee, G., & Kim, B. S. (2014). Biological reduction of graphene oxide using plant leaf extracts. *Biotechnology Progress, 30*, 463–469.
Li, S., Shen, Y., Xie, A., Yu, X., Qiu, L., Zhang, L., et al. (2007). Green synthesis of silver nanoparticles using *Capsicum annuum* L. extract. *Green Chemistry, 9*, 852–858.
Li, J., Cai, C., Yang, C., Li, J., Sun, T., & Yu, G. (2019). Recent advances in pharmaceutical potential of brown algal polysaccharides and their derivatives. *Current Pharmaceutical Design, 25*, 1290–1311.
Malyarenko, O. S., & Ermakova, S. P. (2017). Fucoidans: Anticancer activity and molecular mechanisms of action. In J. Venkatesan, S. Anil, & S.-K. Kim (Eds.). *Seaweed polysaccharides: Isolation, biological and biomedical applications* (pp. 175–203). Amsterdam: Elsevier.
Malyarenko, O. S., Usoltseva, R. V., Shevchenko, N. M., Isakov, V. V., Zvyagintseva, T. N., & Ermakova, S. P. (2017). *In vitro* anticancer activity of the laminarans from Far Eastern brown seaweeds and their sulfated derivatives. *Journal of Applied Phycology, 29*, 543–553.
Maneerung, T., Tokura, S., & Rujiravanit, R. (2008). Impregnation of silver nanoparticles into bacterial cellulose for antimicrobial wound dressing. *Carbohydrate Polymers, 72*, 43–51.
Martinez-Castanon, G., Nino-Martinez, N., Martinez-Gutierrez, F., Martinez-Mendoza, J., & Ruiz, F. (2008). Synthesis and antibacterial activity of silver nanoparticles with different sizes. *Journal of Nanoparticle Research, 10*, 1343–1348.
Medina, C. D., Tien-Street, W., Zhang, B., Huang, X., Vernet, C. A., Nieto-Argüello, A., et al. (2019). Citric juice-mediated synthesis of tellurium nanoparticles with antimicrobial and anticancer properties. *Green Chemistry, 21*, 1982–1988.
Meire, M., Coenye, T., Nelis, H., & De Moor, R. (2012). Evaluation of Nd: YAG and Er: YAG irradiation, antibacterial photodynamic therapy and sodium hypochlorite treatment on *Enterococcus faecalis* biofilms. *International Endodontic Journal, 45*, 482–491.
Menshova, R. V., Shevchenko, N. M., Imbs, T. I., Zvyagintseva, T. N., Malyarenko, O. S., Zaporoshets, T. S., et al. (2016). Fucoidans from brown alga*Fucus evanescens*: structure and biological activity. *Frontiers in Marine Science, 3*, 129.
Morones, J. R., Elechiguerra, J. L., Camacho, A., & Ramirez, J. T. (2005). The bactericidal effect of silver nanoparticles. *Nanotechnology, 16*, 2346–2353.
Onditi, M., Bosire, G., Changamu, E., & Ngila, C. (2019). Degradation of rhodamine B dye by cactus polysaccharide-synthesized silver nanoparticles monitored by fluorescence excitatione-emission matrix (FEEM) spectroscopy. *Starch, 71*, 5–6.
Paknejadi, M., Bayat, M., Salimi, M., & Razavilar, V. (2018). Concentration- and time-dependent cytotoxicity of silver nanoparticles on normal human skin fibroblast cell line. *Iranian Red Crescent Medical Journal, 20*(10), e79183.
Pal, S., Tak, Y. K., & Song, J. M. (2007). Does the antibacterial activity of silver nanoparticles depend on the shape of the nanoparticle? A study of the gram-negative bacterium *Escherichia coli*. *Applied and Environmental Microbiology, 73*, 1712–1720.
Rai, M., Deshmukh, S., Ingle, A., & Gade, A. (2012). Silver nanoparticles: the powerful nanoweapon against multidrug-resistant bacteria. *Journal of Applied Microbiology, 112*, 841–852.
Rodriguez-Sanchez, L., Blanco, M. C., & Lopez-Quinetela, M. A. (2000). Electrochemical synthesis of silver nanoparticles. *The Journal of Physical Chemistry B, 104*, 9683.
Sahayaa, K., Rajesh, S., & Rahi, J. M. (2012). Silver nanoparticles biosynthsis using marine algae *Padina pavonica* (Linn.) and its microbicidal activity. *Digest Journal of Nanomaterials and Biostructures, 7*, 1557–1567.
Saifuddin, N., Wong, C. W., & Nur Yasumira, A. A. (2009). Rapid biosynthesis of silver nanoparticles using culture supernatants of bacteria with microwave irradiation. *E-Journal of Chemistry, 6*, 61–70.
Sailaja, A. K., Amareshwar, P., & Chakravarty, P. (2011). Different techniques used for the preparation of nanoparticles using natural polymers and their application. *International Journal of Pharmacy and Pharmaceutical Sciences, 3*, 45–50.
Schneidewind, H., Schüler, T., Strelau, K. K., Weber, K., Cialla, D., Diegel, M., et al. (2012). The morphology of silver nanoparticles prepared by enzyme-induced reduction. *Beilstein Journal of Nanotechnology, 3*, 404–414.
Shankar, S. S., Ahmad, A., & Sastry, M. (2003). Geranium leaf assisted biosynthesis of silver nanoparticles. *Biotechnology Progress, 19*, 1627–1631.
Shkryl, Y. N., Veremeichik, G. N., Kamenev, D. G., Gorpenchenko, T. Y., Yugay, Y. A., Mashtalyar, D. V., et al. (2018). Green synthesis of silver nanoparticles using transgenic *Nicotiana tabacum* callus culture expressing silicatein gene from marine sponge *Latrunculia oparinae*. *Artificial Cells, Nanomedicine, and Biotechnology, 46*(8), 1646–1658.
Shrivastava, S., Bera, T., Roy, A., Singh, G., Ramachandrarao, P., & Dash, D. (2007). A review on biosynthesis, characterization and antimicrobial effect of silver nanoparticles of *Moringa olifera* (MO-AgNPs). *Nanotechnology, 18*, 225103.
Singh, J., Dutta, T., Kim, K.-H., Rawat, M., Samddar, P., & Kumar, P. (2018). "Green" synthesis of metals and their oxide nanoparticles: Applications for environmental remediation. *Journal of Nanobiotechnology, 16*, 84.
Socrates, G. (2004). *Infrared and Raman characteristic group frequencies: Tables and charts.* Chichester: Wiley347.
Sokolova, R. V., Ermakova, S. P., Awada, S. M., Zvyagintseva, T. N., & Kanaan, H. M. (2011). Composition, structural characteristics, and antitumor properties of polysaccharides from the brown algae *Dictyopteris polypodioides* and *Sargassum*sp. (Lebanon). *Chemistry of Natural Compounds, 47*, 329–334.
Son, W. K., Youk, J. H., & Park, W. H. (2006). Antimicrobial cellulose acetate nanofibers containing silver nanoparticles. *Carbohydrate Polymers, 65*, 430–434.
Sondi, I., & Salopek-Sondi, B. (2004). Silver nanoparticles as antimicrobial agent: A case study on *E. coli* as a model for gram-negative bacteria. *Journal of Colloid and Interface Science, 275*, 177–182.
Tiwari, A., Sherpa, Y. L., Pathak, A. P., Singh, L. S., Gupta, A., & Tripathi, A. (2019). One-pot green synthesis of highly luminescent silicon nanoparticles using *Citrus limon* (L.) and their applications in luminescent cell imaging and antimicrobial efficacy. *Materials Today Communications, 19*, 62–67.
Tummalapalli, M., Deopura, B. L., Alam, M. S., & Gupta, B. (2015). Facile and green synthesis of silver nanoparticles using oxidized pectin. *Materials Science and Engineering C, 50*, 31–36.
Usoltseva, R. V., Shevchenko, N. M., Malyarenko, O. S., Anastyuk, S. D., Kasprik, A. E., Zvyagintsev, N. V., et al. (2019). Fucoidans from brown algae Laminaria longipes and Saccharina cichorioides: structural characteristics, anticancer and radiosensitizing activity in vitro. *Carbohydrate Polymers, 221*, 157–165.
Vanaja, M., Gnanajobitha, G., Paulkumar, K., Rajeshkumar, S., Malarkodi, C., & Annadurai, G. (2013). Phytosynthesis of silver nanoparticles by *Cissus quadrangularis*: Influence of physicochemical factors. *Journal of Nanostructure in Chemistry, 3*, 17.
Venkatesan, J., Singh, S. K., Anil, S., Kim, S.-K., & Shim, M. S. (2018). Preparation, characterization and biological applications of biosynthesized silver nanoparticles with chitosan-fucoidan coating. *Molecules, 23*, 1429.
Venkatpurwar, V., & Pokharkar, V. (2011). Green synthesis of silver nanoparticles using marine polysaccharide: Study of in-vitro antibacterial activity. *Materials Letters, 65*, 999–1002.
Venugopal, K., Ahmad, H., Manikandan, E., Thanigai, A. K., Kavitha, K., Moodley, M. K.,

et al. (2017). The impact of anticancer activity upon *Beta vulgaris* extract mediated biosynthesized silver nanoparticles (ag-NPs) against human breast (MCF-7), lung (A549) and pharynx (Hep-2) cancer cell lines. *Journal of Photochemistry and Photobiology B, Biology, 173*, 99–107.

Zhang, W., Xu, W., Li, J., Liu, H., Li, Y., Lou, Y., et al. (2018). Comparative catalytic and bacteriostatic properties of silver nanoparticles biosynthesized using three kinds of polysaccharide. *AIP Advances, 8*, 065222.

Zvyagintseva, T. N., Shevchenko, N. M., Nazarenko, E. L., Gorbach, V. I., Urvantseva, A. M., Kiseleva, M. I., et al. (2003). Water-soluble polysaccharides of some far-eastern brown seaweeds. Distribution, structure, and their dependence on the developmental conditions. *Journal of Experimental Marine Biology and Ecology, 294*, 1–13.